crystallization communications

Purification, crystallization and preliminary X-ray analysis of adenylosuccinate synthetase from the fungal pathogen *Cryptococcus neoformans*

Ross D. Blundell,[a] Simon J. Williams,[a,b] Carl A. Morrow,[a] Daniel J. Ericsson,[a,b] Bostjan Kobe[a,b]* and James A. Fraser[a]*

[a]Australian Infectious Diseases Research Centre, School of Chemistry and Molecular Biosciences, The University of Queensland, Brisbane, QLD 4072, Australia, and [b]Institute for Molecular Bioscience, The University of Queensland, Brisbane, QLD 4072, Australia

Correspondence e-mail: b.kobe@uq.edu.au, jafraser@uq.edu.au

With increasingly large immunocompromised populations around the world, opportunistic fungal pathogens such as *Cryptococcus neoformans* are a growing cause of morbidity and mortality. To combat the paucity of antifungal compounds, new drug targets must be investigated. Adenylosuccinate synthetase is a crucial enzyme in the ATP *de novo* biosynthetic pathway, catalyzing the formation of adenylosuccinate from inosine monophosphate and aspartate. Although the enzyme is ubiquitous and well characterized in other kingdoms, no crystallographic studies on the fungal protein have been performed. Presented here are the expression, purification, crystallization and initial crystallographic analyses of cryptococcal adenylosuccinate synthetase. The crystals had the symmetry of space group $P2_12_12_1$ and diffracted to 2.2 Å resolution.

1. Introduction

With the rise of the HIV/AIDS pandemic and the increased use of immunosuppressive drugs in chemotherapy and organ transplantation, populations of individuals with defective immune systems are higher than ever before. With such a large immunocompromised population, opportunistic infections are a growing cause of morbidity and mortality. Among these opportunists is the fungus *Cryptococcus neoformans*, one of the foremost AIDS-defining illnesses. Infection by this basidiomycete yeast begins with the inhalation of spores or desiccated yeast cells (Idnurm *et al.*, 2005). Individuals with healthy immune systems generally clear infection by *C. neoformans*. However, in immunocompromised individuals the fungus can disseminate to the central nervous system to cause cryptococcal meningoencephalitis, which is fatal if untreated (Idnurm *et al.*, 2005).

Fungal infections are difficult to treat owing to the similarities of their eukaryotic physiology to that of humans; the limited antifungal agents available tend to target the few differences between the two systems (Odds *et al.*, 2003). Azoles (such as fluconazole) and polyene compounds (such as amphotericin B) target ergosterol by inhibiting the enzyme involved in its biosynthesis (lanosterol 14 α-demethylase) or by binding to ergosterol itself, respectively. New agents of this class are frequently reported; however, few see active clinical development (Ostrosky-Zeichner *et al.*, 2010). Sordarins, which inhibit protein synthesis *via* elongation factor 2 (Domínguez & Martín, 1998), and echinocandins, which inhibit fungal cell-wall glucan synthesis (Emri *et al.*, 2013), both show promise as antifungal agents, but few specific candidates for further trials have emerged (Ostrosky-Zeichner *et al.*, 2010). Considering the current shortage of new drug candidates in the antifungal pipeline, the discovery and development of novel fungal-specific compounds need to be given a high priority. One approach to achieve this is to apply rational drug-design techniques towards fungal-specific aspects of otherwise conserved metabolic pathways.

The purine-metabolic pathway has for over half a century served as a source of targets for therapeutic compounds, including antitumour drugs, immunosuppressants and antivirals (Elion, 1989). Previous studies by our group have shown that purine metabolism is a potential source of antifungal drug targets to combat *C. neoformans* infection (Morrow *et al.*, 2010, 2012). We have already characterized a crucial enzyme in the purine-biosynthesis pathway in this organism, inosine monophosphate dehydrogenase (IMPDH). IMPDH is the

crystallization communications
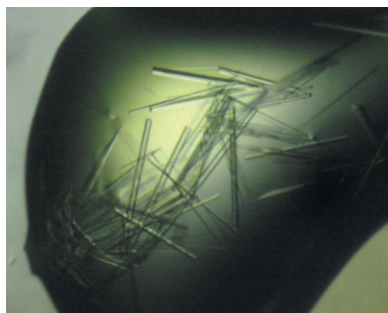
first committed step in *de novo* GTP biosynthesis, catalyzing the conversion of inosine monophosphate (IMP) to xanthosine monophosphate (XMP). Loss of IMPDH activity, and consequently *de novo* GTP biosynthesis, results in death of the pathogen, suggesting that this pathway may be a viable antifungal target (Morrow *et al.*, 2012). To further probe this pathway for targets, we have investigated other purine-biosynthetic enzymes.

Just as IMPDH catalyzes the first step in GTP biosynthesis from IMP, the first step in the conversion of IMP to ATP is governed by the enzyme adenylosuccinate synthetase (AdSS). AdSS catalyzes the formation of adenylosuccinate (S-AMP) from IMP and aspartate. This GTP- and Mg^{2+}-dependent reaction proceeds *via* two steps: firstly, the γ-phosphate from GTP is transferred to the 6-oxygen of IMP, forming the intermediate 6-phosphoryl IMP (6-PIMP); secondly, the 6-phosphoryl group is displaced by the α-amino group of aspartate to form adenylosuccinate (Lieberman, 1956; Fig. 1). Structural studies in *Escherichia coli* and other organisms have shown that the enzyme forms a dimer, with each subunit contributing an arginine residue to the active site of the other molecule (Poland *et al.*, 1993; Silva *et al.*, 1995; Moe *et al.*, 1996; Eaazhisai *et al.*, 2004). In the absence of its substrate, the active site of AdSS is disordered; however, upon ligand binding the substrate-binding pocket and dimer formation are stabilized (Wang *et al.*, 1995; Hou *et al.*, 2002).

With the exception of mature red blood cells, AdSS is an essential enzyme in all organisms studied so far and most cell types (Honzatko & Fromm, 1999; Hou *et al.*, 2002). An alternative route of ATP biosynthesis is the conversion of adenine salvaged from the environment to adenosine monophosphate (AMP). This reaction is governed by the enzyme adenine phosphoribosyl transferase (APRT), which has been characterized in several organisms, including the fungus *Saccharomyces cerevisiae* (Alfonzo *et al.*, 1997). *C. neoformans* carries a predicted APRT-encoding gene (strain H99; CNAG_02858, Broad Institute of MIT and Harvard; http://www.broadinstitute.org/annotation/genome/cryptococcus_neoformans/MultiHome.html).

AdSS has been purified and characterized from several sources. AdSS from *E. coli* is arguably the best characterized (Silva *et al.*, 1995; Poland *et al.*, 1996; Choe *et al.*, 1999) and has 42% identity to the cryptococcal enzyme. Crystal structures are also available for the proteins from *Homo sapiens* (54% identity; PDB entry 2v40; Structural Genomics Consortium, unpublished work), *Mus musculus* (54% identity; Iancu *et al.*, 2001, 2002), the bacteria *Yersinia pestis* (42% identity; PDB entry 3hid; R. Zhang, M. Zhou, S. Peterson, W. Anderson & A. Joachimiak, unpublished work), *Campylobacter jejuni* (43% identity; PDB entry 3r7t; Center for Structural Genomics of Infectious Diseases, unpublished work) and *Burkholderia thailandensis* (40% identity; PDB entry 3ue9; Seattle Structural Genomics Center for Infectious Disease, unpublished work), the plants

Arabidopsis thaliana (55% identity) and *Triticum aestivum* (53% identity; Prade *et al.*, 2000), the eukaryotic parasite *Plasmodium falciparum* (46% identity; Eaazhisai *et al.*, 2004) and the extremophile archaeon *Pyrococcus horikoshii* (33% identity; Wang *et al.*, 2011). The enzyme has been crystallized in the apo form (Silva *et al.*, 1995; Iancu *et al.*, 2001) as well as complexed with various combinations of IMP, GTP, GDP, aspartate, 6-PIMP, Mg^{2+} and two AdSS inhibitors: the antitumour aspartate analogue hadacidin (Kaczka *et al.*, 1962; Tibrewal & Elliott, 2011) and the adenosine 5′-monophosphate-mimicking herbicide hydantocidin (Fonné-Pfister *et al.*, 1996).

To date, there have been no crystallographic studies of AdSS from a fungal species. In the hope that comparison of a fungal AdSS structure with the comprehensive knowledge available from other species may prove useful in the design of future fungal-specific agents, here we describe the crystallization and initial analysis of the crystals of adenylosuccinate synthetase from *C. neoformans*.

2. Materials and methods

2.1. Cloning

Total RNA was isolated from *C. neoformans* var. *grubii* strain H99 using TRIzol (Invitrogen). Intron-free cDNA was then synthesized using a Bioline cDNA synthesis kit (Bioline). The AdSS-encoding gene *ADE*12 (strain H99; CNAG_02858, Broad Institute of MIT and Harvard; http://www.broadinstitute.org/annotation/genome/cryptococcus_neoformans/MultiHome.html) was PCR-amplified, with unique restriction sites (*Bam*HI and *Pst*I) introduced *via* the specifically designed primers UQ2259 (ACGCACGGATCCATGGCTCCATCCCCGGAGGGA) and UQ2260 (GAACGTCTGCAGTTAGAAGATGATAACGTTCTG). The PCR product was then cloned into the TOPO pCR2.1 vector (Invitrogen), sequenced and ligated into *Bam*HI/*Pst*I-cut pQE-30 expression vector (Qiagen), which introduced an N-terminal 6×His tag (MRGSHHHHHHGS).

2.2. Expression and purification

Early failed cloning efforts strongly suggested that the *ADE*12 pQE construct was toxic in *E. coli*. The ligation was therefore transformed into competent BL21(DE3)pLysS *E. coli* cells (Promega) expressing the pREP4 repressor plasmid. Transformed cells were grown in Terrific Broth (TB) medium with 100 µg ml^{-1} ampicillin, 35 µg ml^{-1} kanamycin and 12.5 µg ml^{-1} chloramphenicol. Cultures were incubated at 310 K until they reached an OD_{600} of approximately 1.0, after which they were induced with 1 m*M* IPTG and grown at 293 K for 5 h. Cell pellets were harvested and resuspended in lysis buffer (50 m*M* HEPES pH 8, 300 m*M* NaCl, 1 m*M* DTT, 30 m*M* imidazole, 1 m*M* PMSF) and then lysed by sonication. AdSS
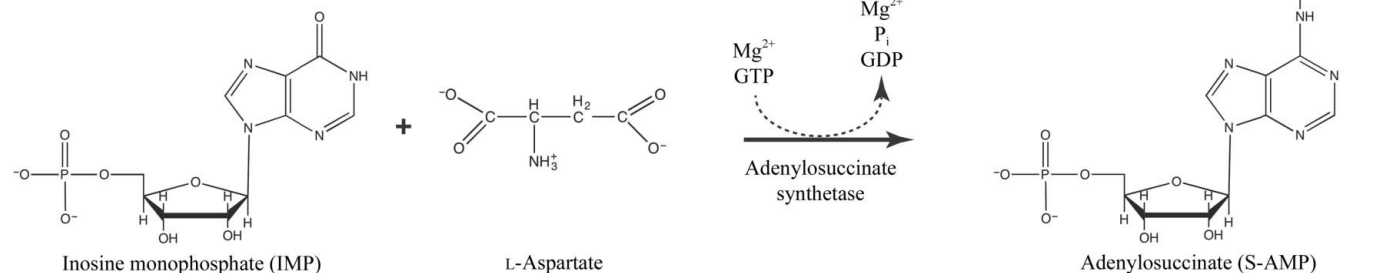

Figure 1
The reaction catalyzed by adenylosuccinate synthetase.

was purified *via* Ni-immobilized metal-affinity chromatography using HisTrap Fast Flow columns (GE Healthcare) and eluted over 20 column volumes in a linear gradient of 30–500 m*M* imidazole. A single main elution peak was seen. Fractions corresponding to this peak were combined and further separated on a Superdex 200 size-exclusion chromatography (SEC) column (GE Healthcare) equilibrated in SEC buffer (10 m*M* HEPES pH 7.5, 150 m*M* NaCl, 1 m*M* DTT) using an ÄKTApurifier FPLC system (GE Healthcare). Peak fractions were combined and concentrated to approximately 16 mg ml^{-1} at >99% purity as estimated by Coomassie-stained SDS–PAGE and snap-frozen for storage at 193 K.

2.3. Crystallization

All crystallization experiments were performed using the hanging-drop vapour-diffusion method at 293 K. Initial screening for crystallization conditions was performed using the Index and PEG/Ion (Hampton Research), PACT premier and JCSG (Qiagen), ProPlex and Morpheus (Molecular Dimensions) and Synergy (Jena Biosciences) commercial screening plates. Plates were set up using a Mosquito Nanodrop crystallization robot (TTP LabTech), with each drop consisting of 100 nl protein solution and 100 nl reservoir solution inverted over 100 µl reservoir solution. A Rock Imager system (Formulatrix) was used to monitor crystal growth in the drops. Crystals were found in approximately 200 conditions. The most promising candidates were chosen for further screening and optimization. Final diffraction-quality crystals were obtained using a condition from the PACT screen. Drops consisting of 1 µl protein solution at 16 mg ml^{-1} and 1 µl reservoir solution (0.1 *M* bis-tris propane pH 8, 0.2 *M* sodium bromide, 17% polyethylene glycol 3350) were streak-seeded from AdSS crystals unsuitable for diffraction after 30 min equilibration over 500 µl reservoir solution. Long rectangular crystals of approximately 0.5 × 0.05 × 0.05 mm formed after 24–48 h (Fig. 2).

2.4. Data collection and processing

Crystals were mounted on nylon loops and treated with a cryoprotectant before being flash-cooled in liquid nitrogen. Initial tests using 20% glycerol in the crystallization solution caused the crystals to shatter, so 15% ethylene glycol was used as a cryoprotectant. X-ray diffraction was performed on the MX2 beamline at the Australian Synchrotron (Clayton, Australia). Reflections were indexed and integrated using *XDS* (Kabsch, 2010) and were then scaled using *AIMLESS* (Evans & Murshudov, 2013) as implemented within the *CCP*4 suite (Winn *et al.*, 2011)
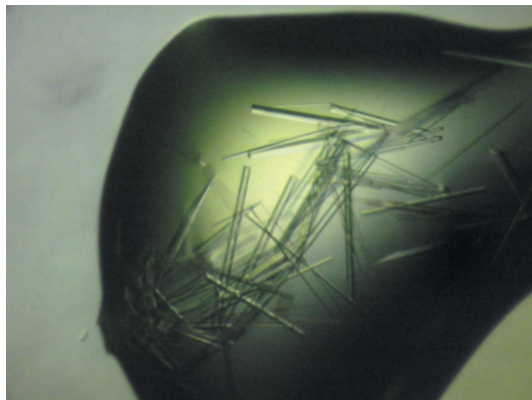

Figure 2
Crystals of adenylosuccinate synthetase from *C. neoformans*, space group *P*2$_1$2$_1$2$_1$.

Table 1
Data-collection and refinement statistics.

Values in parentheses are for the outer shell.

No. of crystals	1
Diffraction source	Australian Synchrotron MX2
X-ray wavelength (Å)	0.95
Detector	ADSC Quantum 315r
Crystal-to-detector distance (mm)	250
Rotation range per image (°)	1
Total rotation range (°)	360
Exposure time per image (s)	2
Data-collection temperature (K)	100
Space group	$P2_12_12_1$
Unit-cell parameters (Å, °)	$a = 58.08$, $b = 101.00$, $c = 163.80$, $\alpha = \beta = \gamma = 90$
Resolution range (Å)	3979.00–2.20 (2.27–2.20)
Unique reflections	49839
Total observations	355630
$\langle I/\sigma(I)\rangle$	19.8 (2.1)
R_{merge}†	0.068 (1.21)
$R_{meas} = R_{r.i.m.}$‡	0.073 (1.415)
Wilson B factor (Å^2)	41.74
Completeness (%)	99.9 (100)
Mosaicity (°)	0.18
Multiplicity	7.3

† $R_{merge} = \sum_{hkl} \sum_i |I_i(hkl) - \langle I(hkl)\rangle| / \sum_{hkl} \sum_i I_i(hkl)$, where $I_i(hkl)$ is the intensity of an individual measurement of the reflection with Miller indices hkl and $\langle I(hkl)\rangle$ is the mean intensity of that reflection. Calculated for $I > -3\sigma(I)$. ‡ $R_{meas} = R_{r.i.m.} = \sum_{hkl} \{N(hkl)/[N(hkl) - 1]\}^{1/2} \sum_i |I_i(hkl) - \langle I(hkl)\rangle| / \sum_{hkl} \sum_i I_i(hkl)$, where $I_i(hkl)$ is the intensity of the ith observation of reflection hkl and $\langle I(hkl)\rangle$ is the weighted average intensity of all observations i of reflection hkl. $N(hkl)$ is the multiplicity.

3. Results and discussion

Full-length His-tagged AdSS from *C. neoformans* was expressed heterologously in soluble form in *E. coli* after 5 h induction at 293 K. Protein appeared as a single band of approximately 46 kDa on reducing SDS–PAGE, matching the estimated size of His-tagged AdSS. During SEC, the protein elutes at 220 ml, which, based on its expected molecular weight and protein calibration standards, suggests a monomeric state in solution. This is in keeping with the established model in which AdSS dimerization is dependent on ligand binding (Kang *et al.*, 1996).

Following the large number of hits obtained from initial sparse-matrix screening, trends in crystallization conditions were investigated. Many hits occurred in conditions using polyethylene glycol 3350 as a precipitant with various types of salts. After comparing the morphologies of these hits, a buffer containing polyethylene glycol 3350 and sodium bromide was chosen. Further rounds of optimization by varying the pH and the PEG concentration and by the addition or absence of glycerol led to large diffraction-quality crystals in 0.1 *M* bis-tris propane pH 8, 0.2 *M* sodium bromide, 17% polyethylene glycol 3350. Protein crystals appeared after 24–48 h at 293 K (Fig. 2). The resolution of the best-diffracting crystals was 2.2 Å. Data-collection and refinement statistics are summarized in Table 1. The crystals are most likely to contain two molecules in the asymmetric unit (corresponding to a Matthews coefficient of 2.61 Å^3 Da^{-1}; Matthews, 1968).

Current work is focusing on solving the structure of AdSS by molecular replacement based on the most similar crystallized homologue (that from *A. thaliana*) as well as obtaining data sets for ligand-bound and inhibitor-bound forms. Analysis of these structures may reveal differences from the human enzyme that could be exploited by structure-based inhibitor design to create leads for new antifungal therapeutics.

crystallization communications

References

Alfonzo, J. D., Sahota, A. & Taylor, M. W. (1997). *Biochim. Biophys. Acta*, **1341**, 173–182.

Choe, J.-Y., Poland, B. W., Fromm, H. J. & Honzatko, R. B. (1999). *Biochemistry*, **38**, 6953–6961.

Domínguez, J. M. & Martín, J. J. (1998). *Antimicrob. Agents Chemother.* **42**, 2279–2283.

Eaazhisai, K., Jayalakshmi, R., Gayathri, P., Anand, R. P., Sumathy, K., Balaram, H. & Murthy, M. R. N. (2004). *J. Mol. Biol.* **335**, 1251–1264.

Elion, G. B. (1989). *Science*, **244**, 41–47.

Emri, T., Majoros, L., Tóth, V. & Pócsi, I. (2013). *Appl. Microbiol. Biotechnol.* **97**, 3267–3284.

Evans, P. R. & Murshudov, G. N. (2013). *Acta Cryst.* D**69**, 1204–1214.

Fonné-Pfister, R., Chemla, P., Ward, E., Girardet, M., Kreuz, K. E., Honzatko, R. B., Fromm, H. J., Schär, H.-P., Grütter, M. G. & Cowan-Jacob, S. W. (1996). *Proc. Natl Acad. Sci. USA*, **93**, 9431–9436.

Honzatko, R. B. & Fromm, H. J. (1999). *Arch. Biochem. Biophys.* **370**, 1–8.

Hou, Z., Wang, W., Fromm, H. J. & Honzatko, R. B. (2002). *J. Biol. Chem.* **277**, 5970–5976.

Iancu, C. V., Borza, T., Choe, J.-Y., Fromm, H. J. & Honzatko, R. B. (2001). *J. Biol. Chem.* **276**, 42146–42152.

Iancu, C. V., Borza, T., Fromm, H. J. & Honzatko, R. B. (2002). *J. Biol. Chem.* **277**, 40536–40543.

Idnurm, A., Bahn, Y.-S., Nielsen, K., Lin, X., Fraser, J. A. & Heitman, J. (2005). *Nature Rev. Microbiol.* **3**, 753–764.

Kabsch, W. (2010). *Acta Cryst.* D**66**, 133–144.

Kaczka, E. A., Gitterman, C. O., Dulaney, E. L. & Folkers, K. (1962). *Biochemistry*, **1**, 340–343.

Kang, C., Kim, S. & Fromm, H. J. (1996). *J. Biol. Chem.* **271**, 29722–29728.

Lieberman, I. (1956). *J. Biol. Chem.* **223**, 327–339.

Matthews, B. W. (1968). *J. Mol. Biol.* **33**, 491–497.

Moe, O. A., Baker-Malcolm, J. F., Wang, W., Kang, C., Fromm, H. J. & Colman, R. F. (1996). *Biochemistry*, **35**, 9024–9033.

Morrow, C. A., Stamp, A., Valkov, E., Kobe, B. & Fraser, J. A. (2010). *Acta Cryst.* F**66**, 1104–1107.

Morrow, C. A., Valkov, E., Stamp, A., Chow, E. W. L., Lee, I. R., Wronski, A., Williams, S. J., Hill, J. M., Djordjevic, J. T., Kappler, U., Kobe, B. & Fraser, J. A. (2012). *PLOS Pathog.* **8**, e1002957.

Odds, F. C., Brown, A. J. & Gow, N. A. (2003). *Trends Microbiol.* **11**, 272–279.

Ostrosky-Zeichner, L., Casadevall, A., Galgiani, J. N., Odds, F. C. & Rex, J. H. (2010). *Nature Rev. Drug Discov.* **9**, 719–727.

Poland, B. W., Hou, Z., Bruns, C., Fromm, H. J. & Honzatko, R. B. (1996). *J. Biol. Chem.* **271**, 15407–15413.

Poland, B. W., Silva, M. M., Serra, M. A., Cho, Y., Kim, K. H., Harris, E. M. S. & Honzatko, R. B. (1993). *J. Biol. Chem.* **268**, 25334–25342.

Prade, L., Cowan-Jacob, S. W., Chemla, P., Potter, S., Ward, E. & Fonne-Pfister, R. (2000). *J. Mol. Biol.* **296**, 569–577.

Silva, M. M., Poland, B. W., Hoffman, C. R., Fromm, H. J. & Honzatko, R. B. (1995). *J. Mol. Biol.* **254**, 431–446.

Tibrewal, N. & Elliott, G. I. (2011). *Bioorg. Med. Chem. Lett.* **21**, 517–519.

Wang, X., Akasaka, R., Takemoto, C., Morita, S., Yamaguchi, M., Terada, T., Shirozu, M., Yokoyama, S., Chen, S., Si, S. & Xie, Y. (2011). *Acta Cryst.* F**67**, 1551–1555.

Wang, W., Poland, B. W., Honzatko, R. B. & Fromm, H. J. (1995). *J. Biol. Chem.* **270**, 13160–13163.

Winn, M. D. *et al.* (2011). *Acta Cryst.* D**67**, 235–242.